Advances in Aircraft and Spacecraft Science, *Vol. 3, No. 4 (2016) 427-445*
DOI: http://dx.doi.org/10.12989/aas.2016.3.4.427

Design modification and structural behavior study of a CFRP star sensor baffle

M. Vinyas*[1], M. Vishwas[2], C.S. Venkatesha[1] and G. Srinivasa Rao[3]

[1]*UBDTCE, Davangere 577004, Karnataka, India*
[2]*Siddaganga Institute of Technology, Tumkur, Karnataka, India*
[3]*Scientist-Engineer, ISRO, Bangalore, Karnataka, India*

(Received December 26, 2015, Revised April 1, 2016, Accepted April 12, 2016)

Abstract. Star sensors are the attitude estimation sensors of the satellite orbiting in its path. It gives information to the control station on the earth about where the satellite is heading towards. It captures the images of a predetermined reference star. By comparing this image with that of the one captured from the earth, exact position of the satellite is determined. In the process of imaging, stray lights are eliminated from reaching the optic lens by the mechanical enclosures of the star sensors called Baffles. Research in space domain in the last few years is mainly focused on increased payload capacity and reduction in launch cost. In this paper, a star sensor baffle made of Aluminium is considered for the study. In order to minimize the component weight, material wastage and to improve the structural performance, an alternate material to Aluminium is investigated. Carbon Fiber Reinforced Polymer is found to be a better substitute in this regard. Design optimisation studies are carried out by adopting suitable design modifications like implementing an additional L-shaped flange, Upward flange projections, downward flange projections etc. A better configuration of the baffle, satisfying the design requirements and achieving manufacturing feasibility is attained. Geometrical modeling of the baffle is done by using UNIGRAPHICS-Nx7.5® . Structural behavior of the baffle is analysed by FE analysis such as normal mode analysis, linear static analysis, and linear buckling analysis using MSC/PATRAN® , MSC-NASTRAN® as the solver to validate the stiffness, strength and stability requirements respectively. Effect of the layup sequence and the fiber orientation angle of the composite layup on the stiffness are also studied.

Keywords: FE analysis; carbon fiber reinforced polymer; design optimisation

1. Introduction

For any space mission to be successful it is necessary to guide the satellite to revolve in the right orbit and gather all the required data without any flaws. Among the many spacecraft subsystems contributing in this regard, Star sensors are the attitude estimation sensors installed in the satellites in order to determine the exact location of the satellite. It helps to bring back the satellite to the required position if there is any deviation from its path. Star sensor captures the image of any of the predetermined reference star. This image is compared with that of the image of the same star captured from the Earth. By this comparison and with the help of star catalogs,

*Corresponding author, Ph.D., E-mail: vinyas.mahesh@gmail.com

http://www.techno-press.org/?journal=aas&subpage=7 ISSN: 2287-528X (Print), 2287-5271 (Online)

digitizers and microprocessors, the attitude and inclination of the satellite is determined.

During the process of imaging, many stray lights enter the lens of the sensor system, which is undesirable. In order to eliminate those stray lights, a mechanical enclosure which protects the optical components of the star sensors known as "Baffle" is used. Along with ensuring the elimination of the stray lights, it is also necessary that the baffle is light weighted and meet the design requirements specified for the mission.

Recent developments in the space research emphasize simple, light weighted design of the spacecraft components in order to reduce the mission cost and improve the performance of the space shuttle. In case of star sensors, care must be taken to avoid swamping starlight with these sources of stray light.

Stray light can be reduced by judicious design of the baffle. In order to obtain the required signal to noise ratio (S/N) under the circumstance that has bright unwanted lights in the vicinity, the control and suppression of stray lights are essential for the observation.

An effective baffle design is necessary to eliminate the unwanted lights during imaging. The different forms of stray lights acting on the baffle are classified by Mohammadnejad *et al.* (2012) as light inside the system, outside the system and light used for imaging. Many researchers have worked on optimizing the Baffle design. Among them, Samaan *et al.* (2012) designed a primary attitude star sensor which resulted in increased star identification success rate. Chao *et al.* (2011) recommended the design must ensure the light does not encounter the lens directly. By providing maximum number reflections for these stray lights inside the baffle surface, better performance can be attained. Cannata *et al.* (2011) has adopted a unique baffle -screw stepped design, to maximize the total internal reflection of incident light and to attain flexibility of the focal length. Zeh *et al.* (2008) designed a reflective baffle for the thermal infrared imaging spectrometer MERTIS which makes use of the optical properties of conic sections of revolution like spheroid and ellipsoid. Jean-Marc Defise (2002) designed a baffle based on the field of view required. Sharma (2012) has studied the performance of the baffle for the stray light actuation and design optimisation is carried out. The stray light restrained by the baffle depends on the included and shielded angle (Zhao *et al.* 2012).

Since weight reduction is the area of concern while designing a spacecraft component, material with high specific stiffness and specific strength has to be used. Earlier Beryllium, Aluminium was used for space craft materials (Murray *et al.* 1991). Yan *et al.* (2011) found that the thin walled baffles satisfied the space-based camera engineering practical needs along with saving the weight. Jia *et al.* (2008) and Zhang *et al.* (2012, 2011) optimised the baffle based on Finite element methods and found Composites are best materials. Pfeiffer (2007) in his work suggested that replacing the conventional space craft materials by the composites, very high mass reduction can be achieved. Lin *et al.* (2007) investigated the performance of carbon fiber composites in space environment and has found it effective. Quaresimin *et al.* (2013) in his investigation emphasizes the importance of layup sequence and thickness of composites to avoid delamination under various loading. The baffle needs to be structurally stable throughout the mission along with meeting the specified design requirements. Guan *et al.* (2011) analysed for the dynamic characteristics of the baffle and structural parameters were optimised.

In this work, the basic principles involved in the design and optimisation of the star sensor baffle is studied. The existing star sensor baffle made of Aluminium is considered for the investigation. Since reduction in weight of Spacecraft structures helps in increase of payload capacity, reducing launching costs, materials used for Spacecraft application must be light in weight and retain their strength and stiffness throughout the mission. This research involves

investigation of an alternate material for Aluminium and Optimizing the existing baffle configuration using Finite Element methods. The goal is to meet the specified stiffness, strength and stability requirements. Various design modifications have been incorporated in the model using 3D modeling. The design requirements of the mission are validated through FE analysis. Parametric study of the composite layup is carried out to obtain an optimum performance. In free vibration analysis (stiffness analysis) the natural frequency and mode shapes of the baffle are obtained; Linear Static analysis (strength analysis) is carried out for the given load cases to determine Hoffmann failure index, Strength Ratio, Margin of Safety and gravity deformation plots of the baffle. Linear buckling analysis (stability analysis) is carried out to determine buckling factors.

2. Methodology

Material with high specific strength, high specific stiffness and low density is investigated theoretically from the available literature, as a substitute for Aluminium. The performance of the selected material is validated through FE analysis (Normal mode analysis). The 3D model of the baffle is created which is later converted to a FE model Meshing is done using CQUAD4 elements with a mesh size of 4 mm. The required material properties (i.e., Aluminium or CFRP) are implemented to the model. FE model is verified for the free boundaries and free edges. Quality of surface elements is maintained as per standards. Important quality issues are Aspect Ratio, Jacobian, Skew Angle, Warpage. Fixed boundary conditions are enforced at the positions specified in the sketch with the help of RBE2 coupling. Inertia load of 50 gravity are applied as per the requirement. Normal mode analysis, linear static analysis and Linear Buckling analysis are performed to validate stiffness, strength and stability of the baffle respectively

2.1 Design requirements

- The design requirements specified for the space environment is as follows
- The stiffness requirement - 1st natural frequency must be ≥150 Hz.
- The mass requirement- 25% less compared to existing.
- Inertial load capacity- 50 gravity.
- Stability requirement- Buckling factor more than 2
- Strength requirement- The failure indices ≤1.
- The margin of safety (MoS)>0.3 for composites

2.2 Details of the existing Baffle design and Validation

The Baffle geometry such as overall length, inner and outer diameters, intermediate vanes positions are shown in Fig. 1. Fig. 2 and Fig. 3 depicts the 3D model and FE model of the baffle. The physical constraints are transformed to the FE model through RBE2 coupling as shown in Fig. 3(b). The normal mode analysis of the existing Baffle configuration is carried out. Materials properties in Table 1 are incorporated in order to study its 1st natural frequency. The obtained FE natural frequency results are validated with the experimental values. The baffle is excited with the help of vibration shaker and its response is read using Laser vibrometry. Data acquisition system is used to acquire the frequency details of the baffle. From Table 2 the Finite Element and

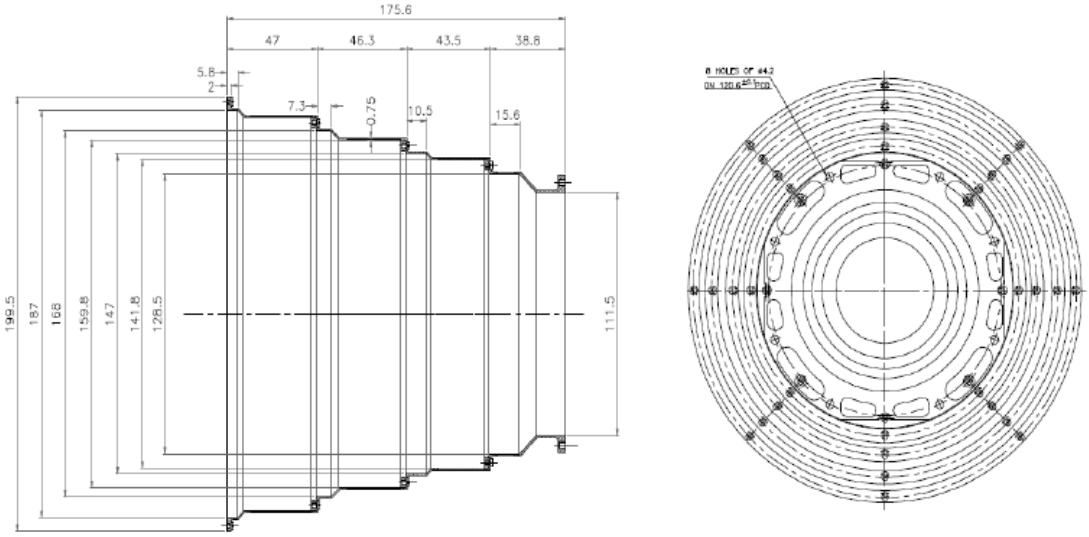

Fig. 1 Sketch of existing baffle

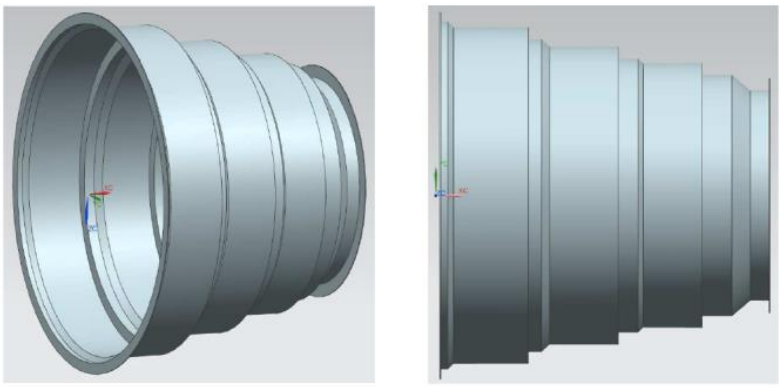

Fig. 2 3D model of the existing baffle

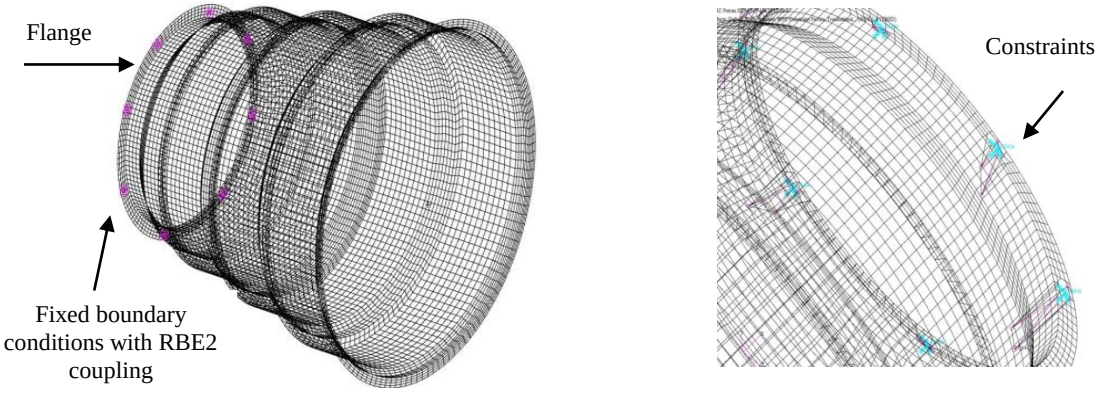

(a) Flange projection (b) Constraints

Fig. 3 FE model of the existing Baffle

Table 2 Finite element and Experimental 1st natural frequency and Mass of Aluminium Baffle

Parameter	Finite Element	Experimental	Error (%)
Frequency (Hz)	382	369	3.43
Mass (Kg)	0.26	0.25	3.84

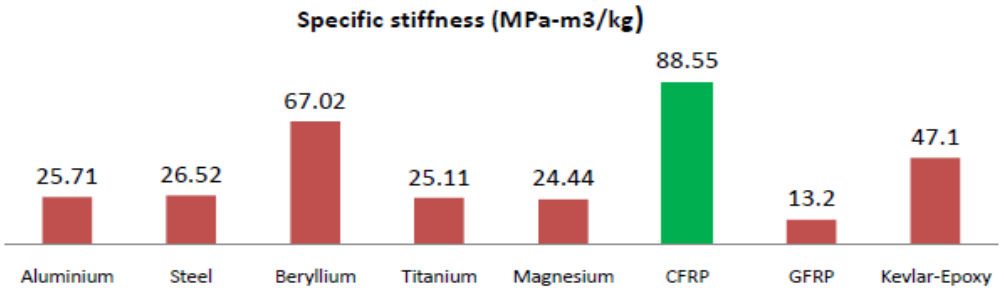

(a) Specific stiffness

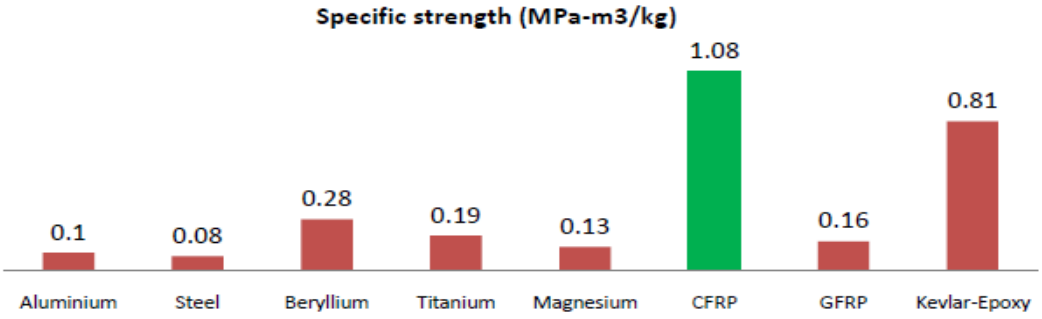

(b) Specific strength

Fig. 4 Comparison of spacecraft materials

Experimental values of stiffness and mass of the baffle are in close agreement. Hence the adopted procedure of Numerical analysis can be carried out further.

(a) Drawbacks of using Aluminium

Aluminium results in increased weight per stiffness ratio, material wastage and processing time which in turn adds up to the cost and performance of the component. Hence an alternate material has to be investigated to overcome these drawbacks.

2.3 Material selection

The material for any of the space craft components is selected based on the mechanical properties like Specific stiffness and Specific strength. Increased value of these properties results in stiffer components with a minimum weight. Fig. 4(a) and 4(b) compares the Specific stiffness and Specific strength of the commonly used space craft materials respectively.

CFRP is found to be the best choice to replace Aluminium by the above comparison.

Table 3(a) Material properties of the BD- M18/43090 lamina

Mechanical property	Value
Effective modulus (longitudinal), E_{11}	147 GPa
Effective modulus (transverse), E_{22}	147 GPa
Shear modulus, G_{12}	4.0 GPa
Poisons ratio	0.03
Density	1600 Kg/m^3
Lamina Thickness	0.1 mm

Table 3(b) Strength properties of the BD- M18/43090 lamina

Material	Tensile Strength (N/mm^2)		Compressive strength (N/mm^2)		Shear strength (N/mm^2)
BD 43090/M18	X_t	Y_t	X_c	Y_c	S
	34.6 e7	34.6e7	20.5e7	20.5e7	4.2e7

Table 4 Comparison of Modal frequencies of existing baffle with Aluminium and CFRP as materials

Baffle Material	Thickness (mm)	1st natural frequency(Hz)	MASS (grams)
ALUMINIUM	0.75	382.4	260
CFRP	0.6	483.4	120
% Reduction in mass=54%			

(b) Normal mode analysis CFRP baffle

The baffle material is changed from Aluminium to CFRP. In order to validate our decision, Normal mode analysis of the baffle is carried out keeping every other parameter (boundary conditions, configuration) unchanged. Material properties of CFRP are given in Table 3(a) and Table 3(b). Six laminas each of thickness 0.1 mm are stacked together in order to get the required thickness of 0.6 mm. The layup sequence used is [0/θ/0/θ/0/θ]. Fibre orientation angle is tentatively set to 45 degrees. The stiffness and mass comparison of baffle materials are shown in Table 4.

Hence replacement of Aluminium by CFRP is justified.

3. Design optimization

The existing baffle design with CFRP has following hurdles which results in a cumbersome manufacturing process.

- Difficult ply layup near sharp edges.
- Maintaining the accurate fiber orientation near sharp edges.
- Possibility of fiber breakage at the sharp corners.
- Baffle experiences warpage at sudden cross section change.
- Difficult to design the required tool or mandrel due to its complex shape.
- Interference of the baffle with the tool/mandrel.
- Increased machining time and cost.

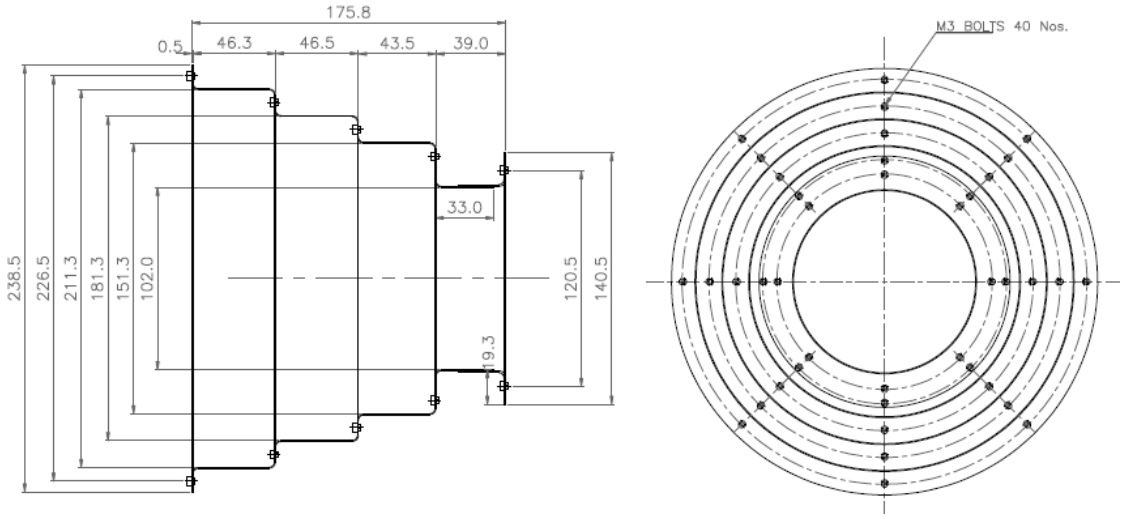

Fig. 5 2D sketch of 1st optimized baffle design

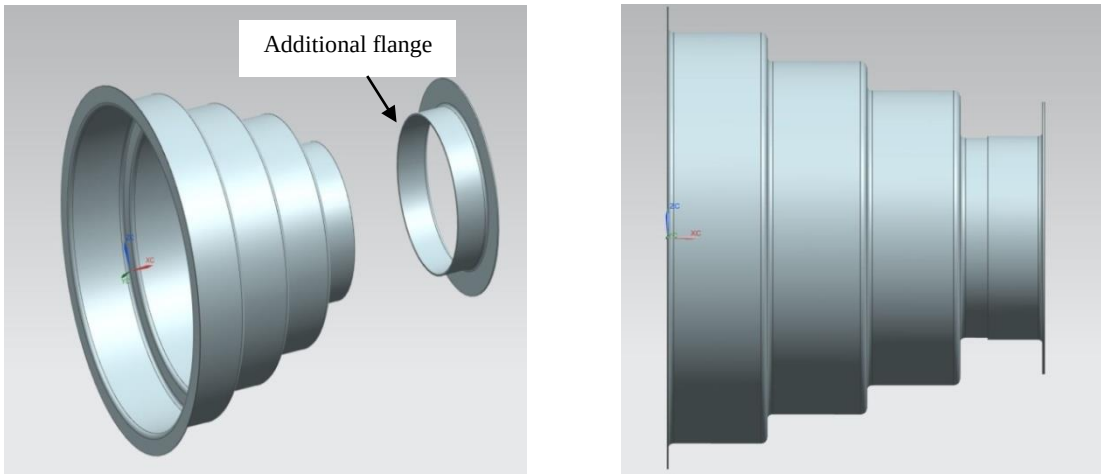

Fig. 6 3D sketch of optimized baffle design-1

3.1 Baffle design-1

The drawbacks in the existing baffle configuration were analyzed and suitable design modifications are made as in Fig. 5 and Fig. 6. It includes,

- Eliminating the narrow sloped cross section, where the ply layups are difficult.
- Sharp corners are removed where the fiber breakage is expected.
- Increasing the diameter of the baffle to incorporate the fillet radius. This ensures easy ply layup and easy removal from the mandrel.
- *L*-section flange is added to improve the root stiffness.

The normal mode analysis of the baffle design-1 is carried out in the same way as described in the previous section. Except the configuration, every other parameter (material, boundary conditions) remains unchanged. Alternate layup sequence $[0/\theta]_n$ (*n*-number of plies) with each

Table 5 Results of the normal mode analysis of 1st optimized design

Trial no.	Layup	Thickness (in mm)	1st natural frequency (in Hz)	Mass (in grams)	% Reduction in mass
1	[0/45/0/45/0/45]	0.6	109	133.4	48.7
2	[0/45/0/45/0/45/0/45]	0.8	143	177.8	31.6

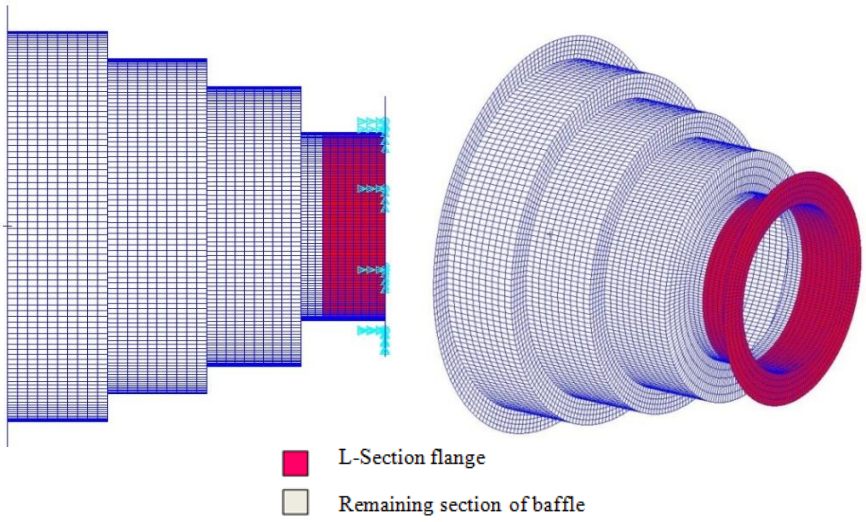

Fig. 7 *L*-section thickness plot

lamina of 0.1 mm thickness is used. The fiber orientation angle of 45 degrees is initially applied.

Results from Table 5 shows that, even though an appreciable mass reduction has been achieved, the specified stiffness requirements are not met.

(c) Optimisation of Baffle design-1 by increasing the L-section Flange thickness

Stiffness improvement is anticipated by strengthening the root of the baffle. Hence the thickness of the root of the baffle (*L*-section flange) is increased compared to other sections of the baffle. Fig. 7 shows the variation in thickness of the baffle. Two trials are carried out with different flange materials to achieve maximum stiffness. Carbon fiber reinforced polymer in the first trial and combination of Carbon fiber reinforced polymer (CFRP) and Aluminium in second.

Trial 1: Using CFRP as flange material.

The normal mode analysis of the baffle is carried out by varying the *L*-section flange (CFRP) thickness, keeping thickness of remaining section of baffle as 0.6 mm as shown in Fig. 7. Effect of flange thickness on 1st natural frequency and mass is shown in Table 6.

Trial 2: Using combination of CFRP and Aluminium as flange material

In the *L*-section, the flange (vertical part) material is changed to aluminium with 2 mm thickness and the material for the horizontal part attached to flange is made using the combination of CFRP (0.6 mm) and aluminium (2 mm) with a total thickness of 2.6 mm as shown in Fig. 8. Results of the stiffness check are illustrated in Table 7.

Table 6 Variation of 1st natural frequency and mass with the thickness of Flange

Trial No.	Material	Thickness of the remaining section of baffle (in mm)	*L*-section thickness (in mm)	1st frequency (in Hz)	Mass (in grams)	% Reduction in mass
1	CFRP	0.6	0.6	109	133.4	48.8
2			2.0	123	172.0	33.8

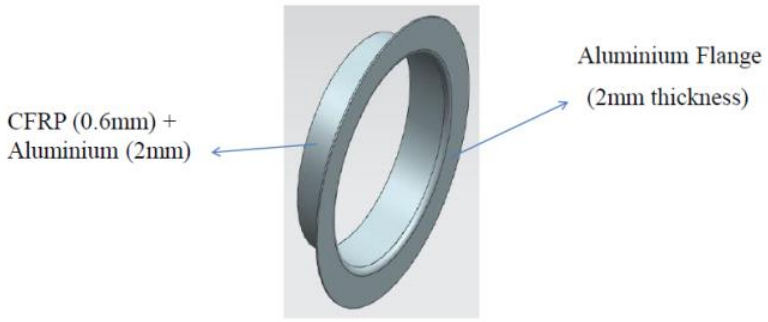

Fig. 8 *L*-Section flange made of Aluminium and CFRP

Table 7 Results of modal analysis for trial 2

L-section configuration	Natural frequency (in Hz)	Mass (in grams)	%Mass reduction
Aluminium flange (2 mm) + (Aluminium+ CFRP=2.6 mm) Near flange	123.03	196	24.6

Table 8 Effect of flange thickness on the 1st natural frequency

Trial No.	Material	Layup sequence	Flange thickness (in mm)	1st frequency (in Hz)	Mass (in grams)	% Reduction in mass
1	CFRP	[0/45/0/45/0/45]*n*	0.6	178.6	144.0	44.6
2			2.0	237.4	159.5	38.6
3			3.0	240.7	170.6	34.6

Inference

Baffle design-1 with additional *L*-section flange made of Aluminium and CFRP materials fails to meet the stiffness requirement. Further increase in thickness of *L*-section flange adds up to the mass, which is undesirable. Hence the design of the baffle has to be refined.

3.2 Baffle design-2

The inability of the Baffle design-1 to meet the requirements are analysed and further modifications are done. They are as follows,

- The additional *L*-section flange has been removed.
- The flange is projected downwards to ease the removal of baffle from the tool.

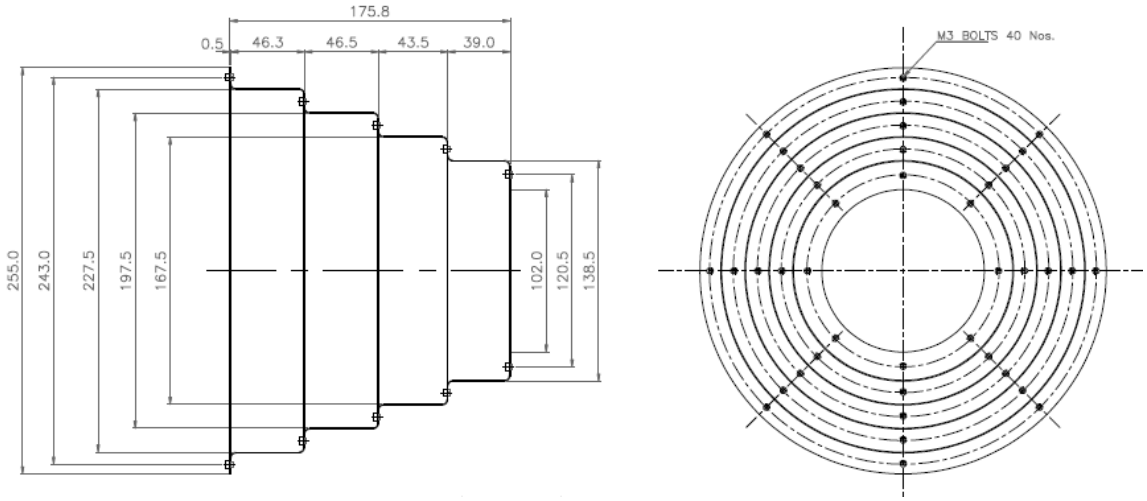

Fig. 9 2D sketch of 2nd optimized baffle design

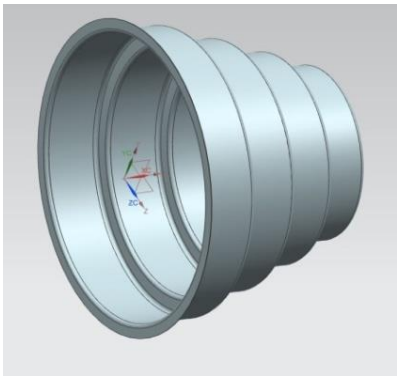

Fig. 10 3D model of the baffle design-2

• The diameter of different sections of the baffle is increased to accommodate the vanes easily.

The 2D sketch and 3D model is shown in Fig. 9 and Fig. 10 respectively. Stiffness check is carried out through modal analysis. In order to study the effect of flange thickness on the 1st natural frequency, it is varied to 2 mm and 3 mm. Thickness of the remaining sections of the baffle is maintained at 0.6 mm.

Results from Table 8 suggest, the design meets the stiffness requirements (179 Hz) and an appreciable amount of mass reduction (44.6%) has been achieved. The optimisation process proceeds to save more weight by reconfiguration of the design.

3.3 Baffle design-3

Since the baffle design-2 satisfies the frequency requirement of 150 Hz, same configuration of the baffle is retained and its dimensions are modified to improve the weight reduction and frequency. Decreasing the diameter of the baffle at different sections results in preventing the extra material adding up to the mass and makes the structure stiffer. The 2D sketch is depicted in Fig. 11.

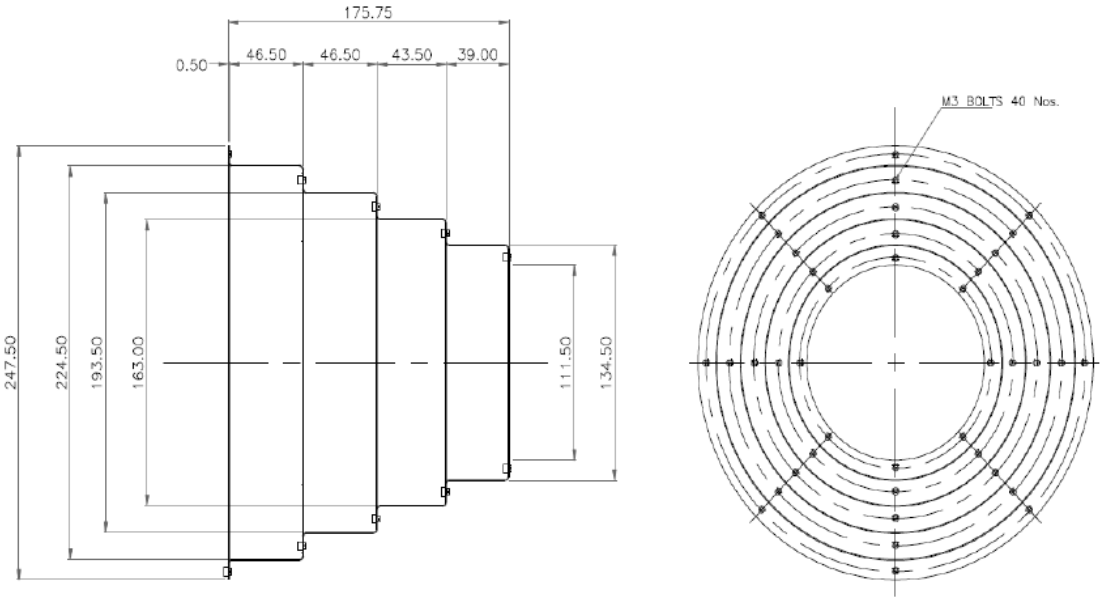

Fig. 11 2D sketch of 3rd optimized baffle design

Table 9 1st natural frequency and mass reduction for various flange thickness

Trial No.	Material	Layup	Flange thickness (in mm)	1st frequency (in Hz)	Mass (in grams)	% Reduction in mass
1			0.6	225	137.0	47.3
2	CFRP	[0/45/0/45/0/45]	2.0	256	147.1	43.5
3			3.0	257	155.2	40.3

Table 10 Effective modal mass matrix

Mode no.	Frequency (in Hz)	T1 (kg)	T2 (kg)	T3 (kg)	R1 (kg-m^2)	R2 (kg-m^2)	R3 (kg-m^2)
1	224	2.4 E-06	9.97E-03	3.96E-02	7.6E-13	3.8E-05	9.6E-06
2	230	8.1 E-07	3.86E-02	9.7 E-03	1.22 E-11	1.06 E-05	4.22E-05
3	433	1.06 E-01	2.59 E-09	1.23 E-09	1.78 E-13	7.46E-09	1.71E-08

The results of the Normal mode analysis of the present baffle tabulated in Table 9 suggest that the 1st natural frequency is improved by 47 Hz with an effective mass reduction of 48 percent. Hence this design of the baffle is finalized and further analysis is carried out.

3.4 Modal effective mass

The modal effective mass matrix of the baffle is calculated to validate the mode shapes of the CFRP baffle depicted in Fig. 12. Modes with higher percentage of the effective mass can be instantly excited by base excitation. It is useful in making design modifications and improves the stiffness of the region prone to failure. Table 10 shows the effective modal mass matrix of the

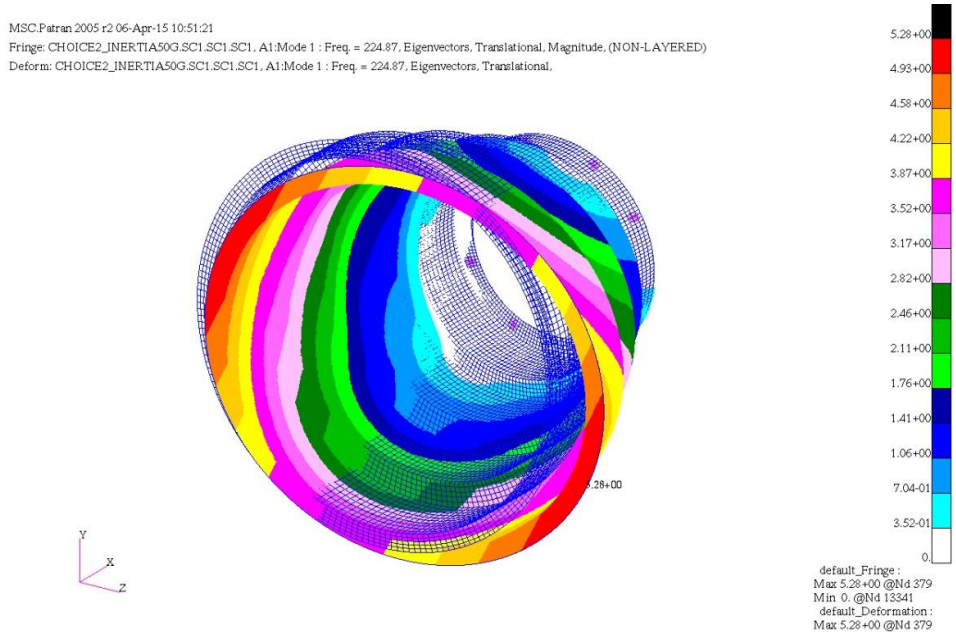

(a) 1st mode- *Z*-direction

(b) 2nd mode- *Y*-direction (c) 3rd mode- *X*-direction

Fig. 12 Mode shapes of the Baffle design-3

baffle with 3 translational and 3 rotational degrees of freedom. For the 1st, 2nd and 3rd modes the dominance of translational movement in *Z*, *Y* and *X* direction respectively is observed.

3.5 Parametric study of composite layup

A composite structure is made of two or more lamina bonded together to obtain the required thickness. Each lamina contains fibers oriented along different directions. The maximum stiffness and strength of the lamina is observed along the fiber direction. The layup sequence, ply orientation affects the effective modulus of the composite which in turn determines the stiffness and strength of the component. Till now, all the analysis is carried out with BD 43090/M18 as the material with a layup sequence of [0/45/0/45/0/45]. 6 laminate, each 0.1 mm thick is stacked together to obtain the actual thickness of the baffle (0.6 mm). In this section a parametric study is

carried out to decide the best ply layup with appropriate fiber orientation to meet the strength and stiffness requirement.

(a) Selection of Layup sequence

The characteristics of the composite are dependent on the layup sequence selected. To analyze the effect of ply layup sequence on the stiffness of the baffle, three ply layup fashions are tested with an initial fiber orientation angle as 45 degree. They are given below.

L_1= [0/θ/0/θ/0/θ]

L_2= [0/θ/θ/θ/θ/0]

L_3= [0/θ/0/0/θ/0]

Each layup is adopted for the baffle and normal mode analysis is done to find the better layup sequence in terms of frequency. Fig. 13 shows the comparison of 1st natural frequency, Effective Young's modulus and Effective shear modulus for the three layup sequence selected.

(b) Selection of fiber orientation angle

Once the layup sequence is confirmed, various fiber orientation angles are checked to obtain an optimum value for θ with improved stiffness. For the selected layup format L_3=[0/θ/0/0/θ/0], optimum fiber orientation angle is determined by varying the orientation angle 45° from 0° to 90° in the steps of 10° and normal mode analysis is carried out. The variation in the natural frequency and effective modulus with respect to fiber orientation angle is shown in Table 11.

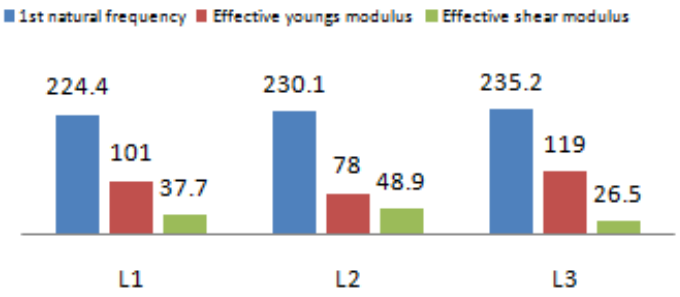

Fig. 13 1st natural frequency, Effective modulus of various Layup sequence

Table 11 1st natural frequency and Effective modulus for different fiber orientation

	FIBER ORIENTATION (in degrees)	f_1 (Hz)	E_{11} (GPa)	E_{22} (GPa)	G_{12} (GPa)
LAY-UP [0/θ/0/0/ θ/0]$_n$	10	231.0	144	144	6.63
	20	233.5	136	136	13.3
	30	234.4	127	127	20.8
	45	235.2	119	119	26.5
	50	234.5	120	120	20.6
	60	234.5	127	127	20.8
	70	233.8	136	136	13.3
	80	231.4	144	144	6.63

Table 12 Failure indices and Strength ratio

Inertial Load	Thickness (mm)	Load Direction	Failure Index	Strength Ratio
50 g	0.6	*X*	0.064	3.95
		Y	0.183	2.33
		Z	0.212	2.15

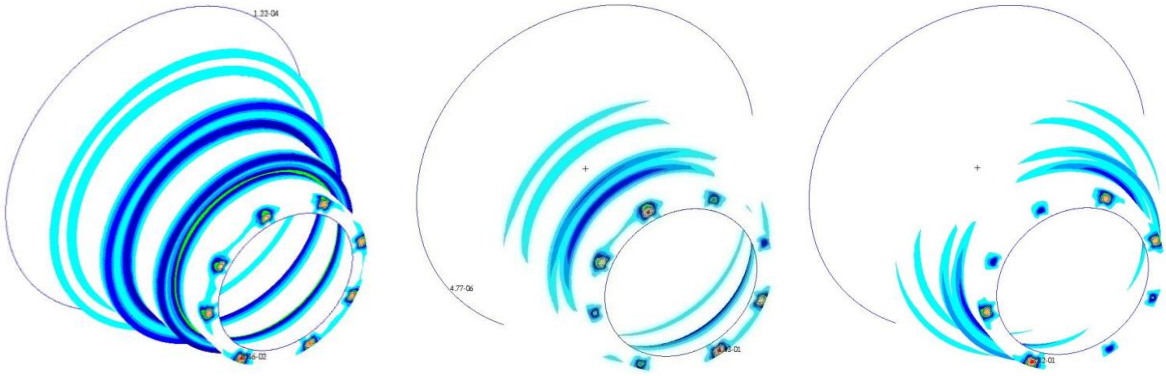

(a) *X*-direction- 0.064 (b) *Y*-direction-0.183 (c) *Z*-direction-0.212

Fig. 14 Maximum failure Indices plots for 50 g

4. Results and discussions: FEA analysis

4.1 Linear static analysis

The space craft structure is subjected to various loading conditions during its launch. Linear static analysis is carried out to ensure sufficient margins for the specific quasi-static loads. NASTRAN 101 solution is used for the linear static analysis of the CFRP baffle. Inertial load of 50 g in *X*, *Y*, *Z* direction is considered as the upper limit of the load acting on the baffle. The strength of the baffle is found by Hoffman failure criteria. Failure indices, Strength ratios (the ratio of the maximum sustainable load to the applied load) and Margin of safety are used in this regard.

(a) Failure indices

The baffle with over all thickness of 0.6 mm is applied with an inertial load of 50 gravity in *X*, *Y*, *Z* directions individually. Failure Index and Strength Ratio are shown in Table 12.

From Table 12 we can observe that the failure index (FI) values are less than 1 and hence the design is safe against the applied load of 50 g. Fig. 14 shows the variation of failure indices at different regions of baffle. The maximum failure index of 0.212 is observed when the baffle is loaded in *Z*-direction and the corresponding strength ratio is 2.15.

(b) Calculation of margin of safety

For a composite structure, the margins of safety (MoS) must be greater than 0.3 to work without failure. From the above analysis, minimum strength of the baffle is observed when it is loaded in *Z*-direction with a SR of 2.15. Hence this factor is considered to calculate the MoS.

The margins of safety (**MoS)** = SR-1 = 2.15-1 =**1.15**>0.3.

Table 13 Single point constraint forces

INERTIAL LOAD	LOAD DIRECTION	SPC FORCES (in N)		
		F_X	F_Y	F_Z
50 g	*X*	9.64	3.02	3.43
	Y	24.9	23.2	13.0
	Z	26.7	12.6	23.3

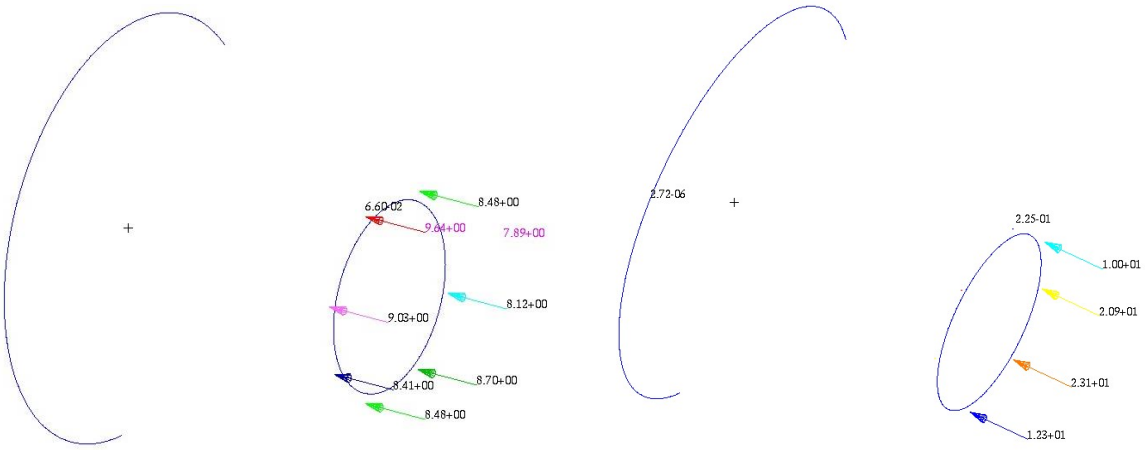

(a) *X*-direction - 9.64N (b) *Y*-direction-24.9

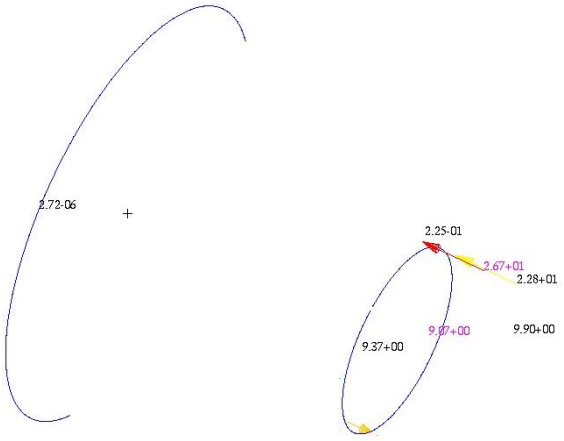

(a) *Z*-direction- 26.7

Fig. 15 Maximum constraint force plots for 50 g

(c) Validation of the joint strength.

From the Linear static analysis the components of the reactional forces for the each case is obtained. The results are summarized in Table 13.

From the Fig. 15 it can be observed that the maximum constraint force of 26.7 N (*X*-component) is found out when an inertial load of 50 g is acting in the *Z*-direction. Hence the threat of failure for the baffle design is expected when loading is in *Z*-direction.

The baffle is attached to its interacting components at its interfaces with the help of M3 bolt. The nut factor of the M3 bolts is considered to be 0.3. In order for the joints to be safe against the slip and separation caused due to the applied load, it is necessary that the reactional forces (SPC forces) at the joints must be less than the preload and the frictional force of the joint.

Calculation of preload

$$\text{Preload=Torque / (Nut factor* Diameter of the bolt)}$$
$$=15 \text{ kgf-cm} / (0.2*0.3)$$
$$= 250 \text{ kgf}$$
$$\text{Preload=2452.5 N> Constraint forces} \quad (1)$$

Calculation of frictional force

$$\text{Frictional force} = \mu * \text{preload}$$
$$= 0.3*2452.5$$
$$\text{Frictional force =735.75 N> Constraint forces.} \quad (2)$$

From Eqs. (1)-(2), it is found that the joints have a sufficient margin against the slip and separation. Hence the joints are safe.

(d) Gravity deformation plots

The CFRP baffle deforms when acted upon gravity load. Analyzing these gravity deformations helps us to analyse the structural design. Fig. 16 shows the deformation plots for 50 gravity load. It can be observed that maximum deformation is experienced at the opening of the baffle.

(e) Inference

From the linear static analysis, it is found that for a baffle with over all thickness of 0.6 mm,

- The failure indices are less than 1.
- The strength ratios are more than a factor of 2.

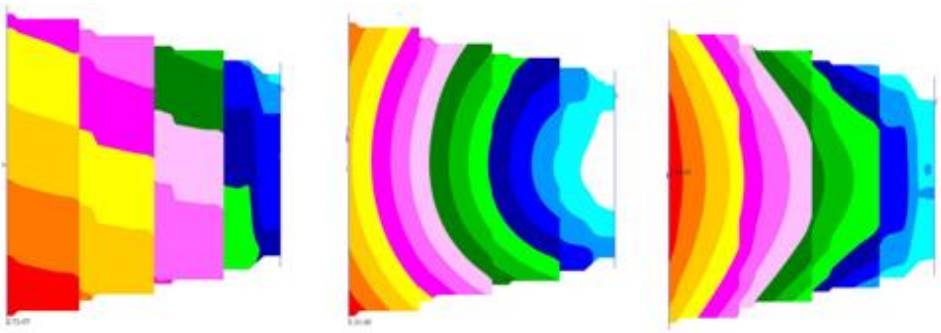

Fig. 16 Deformation plot of CFRP baffle for 50g load- *X*, *Y*, *Z* direction

Table 14 Buckling factors

Inertial load	Baffle Thickness (mm)	Loading direction	Buckling factors
50 g	0.6	*X*	297.16
		Y	169.00
		Z	171.42

• The margin of safety for composites is greater than 0.3

The design meets the strength requirements. Hence it is considered to be safe.

4.2 Linear buckling analysis

The baffle with thickness of 0.6 mm is analyzed for stability using the NASTRAN solution 105. The boundary conditions remain unchanged. The inertia loads of 50 g are applied in *X*, *Y* and *Z* directions independently. The buckling factors for individual loading directions are given in Table 14 and their corresponding buckling shapes in Fig. 17.

(a) Buckling factor plots

(a) *X*- Direction –Buckling factor of 297.16

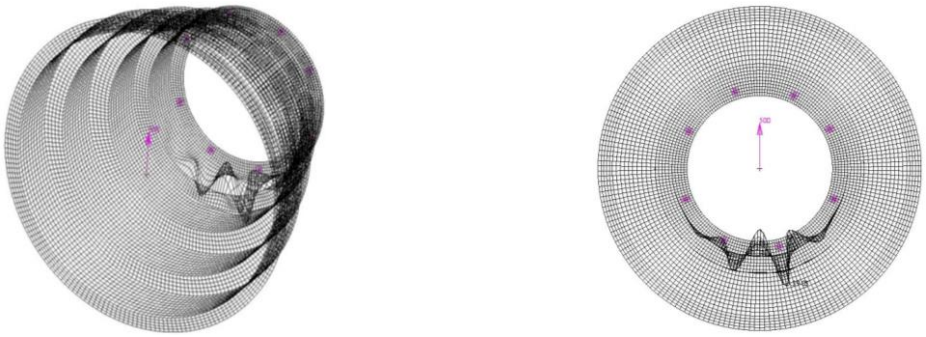

(b) *Y*- Direction –Buckling factor of 169.0

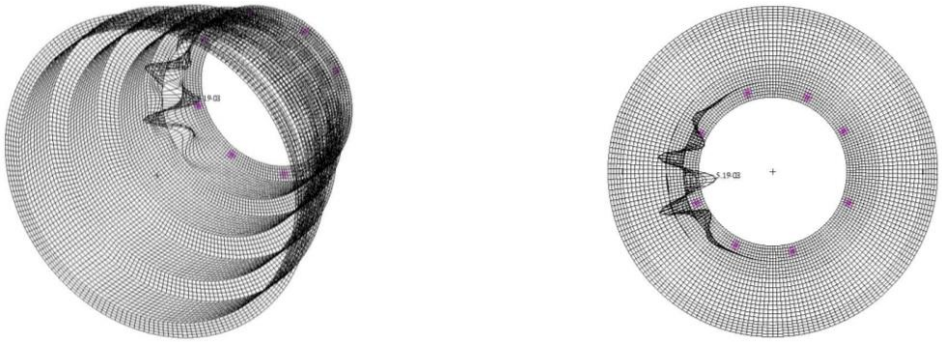

(c) *Z*- Direction –Buckling factor of 171.42

Fig. 17 Buckling analysis plot for 50 g loading

(b) Inference

• The buckling factors are more than 2 for an inertial load of 50 g individually in *X*, *Y* and *Z* directions.
• Minimum stability is observed when the baffle is loaded in *Y*-direction.
• The baffle design meets the stability requirements.

5. Conclusions

The existing star sensor baffle made of Aluminium has been successfully replaced by Carbon fiber reinforced polymer. The normal mode analysis of the baffle with Carbon fiber reinforced polymer (CFRP) justifies the stiffness improvement and mass reduction. Baffle configuration is optimised in order to achieve the manufacturing feasibility along with design requirements. Baffle design-1 and Baffle design-2 failed to fulfil the mission requirements. Proposed Baffle design-3 is found to be the optimum design meeting all the requirements. Parametric analysis of the composite layup suggests an optimum layup sequence of [0/θ/0/0/θ/0] with fiber orientation angle of 45° gives improved stiffness. Linear static analysis of the baffle, applied with 50 gravity loading suggests that the Failure indices are less than 1 and the Margin of safety is greater than 0.3. The joint strength is good enough to avoid slip and separation. Linear buckling analysis results suggest the design is stable enough to bear the load without buckling.

References

Cannata, M.N., Greene, M.R., Mulligan, S.J. and Popovici, V. (2011), "Autonomous star-imaging attitude sensor (ASIAS)", Thesis, York University, NY.

Chao, M., Sizhong, Z., Ming, M., Zhili, G. and Shimin, Z. (2011) "A new method of baffle design", *Procedia Eng.*, **15**, 4516-4520.

Defise, J.M., Halain, J.P., Mazy, E., Rochus, P.P., Howard, R.A., Moses, J.D., ... & Simnett, G.M. (2002), "Design and test of heliospheric imager of the STEREO mission", *Astronomical Telescopes and Instrumentation*, International Society for Optics and Photonics.

Guan, Y., Mu, D. and Li, Z. (2011), "Design and analysis of outer baffle of space telescope", *Appl. Inform. Commun.*, **226**, 477-485.

Lin, Z.W., Liu, Y.Q., Liang, Y., Dong, P., Wang, M.Y. and Li, X.D. (2007), "Application of carbon fibre reinforce composite for space based to space optical structure", *Opt. Precis. Eng.*, **15**, 1181-1185.

Mazy, E., Defise, J.M. and Plesseria, J.Y. (1996), "INTEGRAL optical monitoring camera stray-light design", *Proceedings 2nd INTEGRAL workshop*, The Transparent Universe, St Malo, France.

Mohammadnejad, S. and Madineh, A.B. (2012) "Baffle simulation and design with the aim of use in space cameras", *8th IEEE, IET International Symposium on Communication Systems, Networks and Digital Signal Processing*, July.

Murray, B.W., Floyd, D.R. and Ulph Sr, E. (1991), "Light-absorbing, lightweight beryllium baffle materials", *Proc. SPIE 1485, 88, Reflective and Refractive Optical Materials for Earth and Space Applications*, Orlando, September.

Pfeiffer, K. (2007), *Ultra-Lightweight Optical Baffles out of CFRP*, HPS GmbH Publications.

Quaresimin, M., Ricotta, M., Martello, L. and Mian, S. (2012), "Energy absorption in composite laminates under impact loading", *Compos. Part B*, **44**, 133-140.

Samaan, M. and Theil, S. (2012), "Development of a low cost star tracker for the SHEFEX mission", *Aerosp. Sci. Tech.*, **23**, 469-478.

Sharma, A.K. (2012), "Stray light analysis of optical attitude sensors", *IX Control Instrumentation System Conference (CISCON - 2012)*, 16-17.

Xuezhi, J., Guang, J. and Lei, Z. (2008), "Design and optimization of lightweight outer baffle for space camera", *Opt. Precis. Eng.*, **16**, 1560-1564.

Yan, Y., Song, G., Yuan, A. and Jin, G. (2011), "Optimum design of the carbon fiber thin-walled baffle for the space-based camera", *Proc. SPIE 8196, International Symposium on Photoelectronic Detection and Imaging*, June.

Zeh, T., Gal, C., Kaiser, S., Peter, G., Walter, I., Helbert, J. and Jachlewski, J. (2008), "MERTIS-reflective baffle design and manufacturing", *Proc. SPIE 7808, Infrared Remote Sensing and Instrumentation XVIII*, 78080O.

Zhang, L., Jia, X., Xie, P. and Xing, L. (2012), "Study on ultra-light secondary baffle for coaxial two mirror telescope", *Proceedings of 2012 IEEE, International Conference on Mechatronics and Automation*, Chengdu, August.

Zhang, L., Yao, J., Jia, X. and Jin, G. (2011), "Research on lightweight outer baffle for coaxial space camera", *International Conference on Electronic & Mechanical Engineering and Information Technology*, August.

Zhao, S.F., Wang, H.T., Wang, Y. and Ji, C.Y. (2012), "Space luminous environment adaptability of missile-borne star sensor", *J. Cent. South Univ.*, **19**, 3435-3443.

EC